Ecological Processes

RESEARCH

Open Access

Time lag effect of vegetation response to seasonal precipitation in the Mara River Basin

Shouming Feng[1,2,3], Zhenke Zhang[1,2*], Shuhe Zhao[1,2,3*], Xinya Guo[1,2], Wanyi Zhu[1,2] and Priyanko Das[1,2]

Abstract

Background Mara River Basin is an ecologically fragile area in East Africa, with a pattern of alternating wet and dry seasons shaped by periodic precipitation. Considering the regional biological traits and climatic change, the vegetation's response to seasonal variation is complicated and frequently characterized by time lags. This study analyzed the variation of the Normalized Difference Vegetation Index (NDVI) and investigated its time lag to precipitation at the monthly scale. NDVI characteristic peaks were proposed from the perspective of seasonal mechanisms and were quantified to assess the lag effect.

Results The results showed that the Anomaly Vegetation Index could identify low precipitation in 2006, 2009, and 2017. The NDVI showed an increasing trend in 75% of areas of the basin, while showed a decreased significance in 3.5% of areas, mainly in savannas. As to the time lag, the 1-month lag effect dominated most months, and the spatiotemporal disparities were noticeable. Another method considering the alternations of wet and dry seasons found that the time lag was approximately 30 days. Based on the time distribution of NDVI characteristic peaks, the average time lag was 35.5 days and increased with the range of seasons.

Conclusions The findings confirmed an increasing trend of NDVI in most regions from 2001 to 2020, while the trends were most obvious in the downstream related to human activities. The results could reflect the time lag of NDVI response to precipitation, and the 1-month lag effect dominated in most months with spatial heterogeneity. Four NDVI characteristic peaks were found to be efficient indicators to assess the seasonal characteristics and had a great potential to quantify vegetation variation.

Keywords Mara River Basin, NDVI, Seasonal precipitation, Characteristic peak, Time lag

Introduction

Vegetation in terrestrial ecosystems indicates a variation of regional features due to the interaction between the land surface and atmosphere (Cao and Woodward 1998; Zhang et al. 2013; Jeong et al. 2017). Geospatial differentiation of vegetation is obvious, and regional and seasonal variations have an impact on its growth. Although the surface and climatic conditions that determine different regions vary greatly, the vegetation condition is the most effective and comprehensive indicator of ecosystems (Chamaille-Jammes et al. 2006). The vegetation index can effectively monitor the photosynthetic biomass of plant canopy (Tucker 1979), and depict vegetation productivity and conditions accurately. Former studies concentrated on the seasonal changes of the vegetation index, particularly its association with climate change and anthropogenic activities (Piao and Fang 2003; Jiang et al. 2017). The Normalized Difference Vegetation Index (NDVI) is widely utilized for vegetation monitoring, and its periodic

*Correspondence:
Zhenke Zhang
zhangzk@nju.edu.cn
Shuhe Zhao
zhaosh@nju.edu.cn
[1] School of Geography and Oceanography Sciences, Nanjing University, Nanjing 210023, China
[2] Institute of African Studies, Nanjing University, Nanjing 210023, China
[3] Jiangsu Center for Collaborative Innovation in Geographical Information Resource Development and Application, Nanjing 210023, China

fluctuation reflects the differentiation characteristics of geographical environments.

Due to the impact of surface environments and human activities, NDVI exhibits spatial and temporal fluctuations with seasons (Chamaille-Jammes et al. 2006). Previous research mainly focused on the seasonal changes of vegetation determined by temperature changes (Xu et al. 2013). Since temperature is the primary climatic component, seasons are categorized as spring, summer, autumn, and winter (Jaber et al. 2020). However, in arid and semi-arid areas, precipitation becomes the main climatic factor affecting the inter-annual fluctuation of vegetation (Tang et al. 2017). Random forest algorithms have been used to assess the influence of temperature and precipitation on vegetation greenness trends (Zhu et al. 2022). However, the former study did not quantify the impact or examine how vegetation responds to climate factors, especially the response of vegetation to seasonal precipitation. Studying the relationship between precipitation and vegetation is critical for terrestrial ecosystems (Chen et al. 2020), particularly the spatiotemporal response and lag features of vegetation to seasonal alternation.

The division of seasons caused by precipitation can be categorized as wet and dry. The Mara River Basin (MRB), located on the East African Plateau close to Lake Victoria, exhibits a typical bimodal rainfall pattern. The periodic precipitation shapes the pattern of alternating wet and dry seasons in the MRB, evidently reflected in the seasonal variation of vegetation features. The response of NDVI to the seasonal precipitation is complex and often exists time lags. The variation of NDVI trends exhibits apparent spatial heterogeneity, which is consistent with regional characteristics and climatic change (Pang et al. 2017). A considerable time lag between vegetation and the seasonal precipitation brought on by the climate will occur from the accumulation of climate states, and this lag will exhibit significant spatial heterogeneity (Wen et al. 2019). The time lag effect, essentially based on regression analysis, is used in existing studies to determine the lag of NDVI on climate factors (Zhao et al. 2017). The lag time that corresponds to the highest determination coefficient is thought to be the ideal one.

The time lag effect was analyzed on a large scale in the earlier studies (Wu et al. 2015; He 2019; Kraft et al. 2019), in which spatial resolution was scarce and could not accurately reflect the features at the regional level. The geographical heterogeneity of local regions could not be well predicted by spatial variability at the continental scale. In addition, correlation analysis had not been carried out at a monthly scale, which would generate great spatiotemporal variability. When a constant lag time was applied for all months, the distinctions between months were hidden and the consequences of seasonal changes were completely disregarded. The variation of seasonal precipitation would alter the lag time. The seasonal features of alternation tended to be ignored in previous studies and need to be taken into account from the perspective of seasonal mechanisms.

This study examined the temporal and spatial trends of NDVI. Two methods were adopted to analyze the time lag of NDVI response to seasonal precipitation, which were (1) the correlation analysis and (2) the characteristics of seasonal changes. The time lag of NDVI to seasonal precipitation was calculated at a monthly scale. It was proposed that NDVI showed characteristic peaks during each wet and dry season, which was indicative of vegetation analysis and the time lag effect. In addition, this study analyzed the time lag based on the temporal distribution and characteristics of NDVI peaks. The research overcame the restriction of a constant lag time and indicated the difference in lag time over months. The results considered the seasonal variation, and could better represent the lag time of regional areas with a high spatial resolution. Four NDVI characteristic peaks were proposed, which was helpful to better understand the vegetation characteristics and regular seasonal change. Quantifying time lag based on NDVI characteristic peaks can provide a new perspective on vegetation response to ecological processes.

Study area and data

Study area

The Mara River Basin (MRB) is located in eastern Africa (Fig. 1), spanning Kenya (about 65% of the region) and Tanzania (about 35% of the region), originating in the wetlands of the forested Mau Escarpment. Although it accounts for only about 5% of the water flowing into Lake Victoria, it is one of the most important catchments. The upstream basin (1–4 sub-basins) is heavily forested. The midstream basin (5–9 sub-basins) is covered with savanna, and it flows through wetlands at lower elevations downstream (10–12 sub-basins) to Lake Victoria. The elevation of the basin ranges from 1100 m to over 3000 m, presenting a pattern of high in the east and low in the west. Natural resources, social and cultural heritage, and a rich and original biodiversity are all still retained in the MRB (Dessu 2013). Environmental conservation and biodiversity implications are profound and significant for water-scarce Kenya and Tanzania (Birundu and Mutua 2017).

Precipitation in the MRB varies greatly between seasons and sub-basins. Due to the lack of observation stations, obtaining in situ data on precipitation, temperature, evapotranspiration, and air pressure is difficult. The near meteorological stations in Musoma

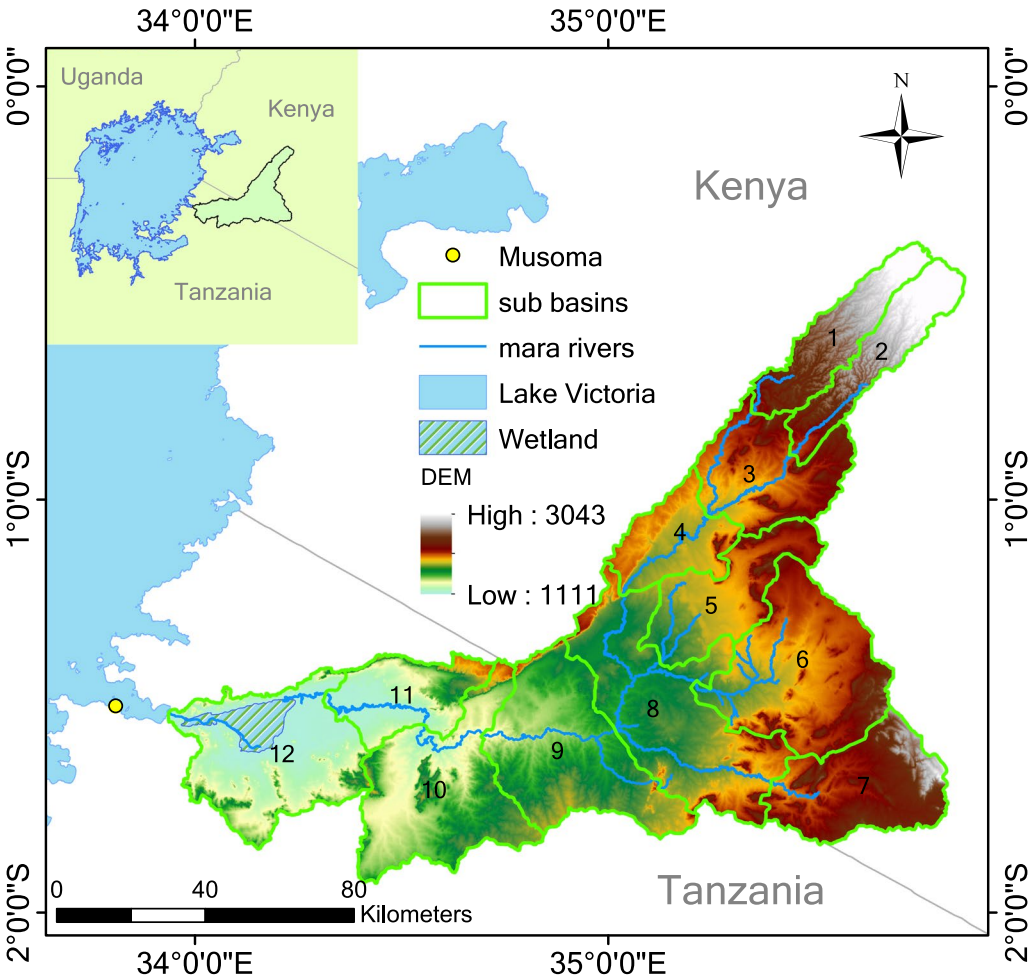

Fig. 1 Location, elevation, sub-basins, and main rivers of the Mara River Basin. The nearest city Musoma is located in the downstream of MRB. The relative positions of the MRB, Lake Victoria, Kenya, and Tanzania are shown in the upper left subgraph

are generally used to characterize the features of MRB. Annual precipitation can reach 1000–1750 mm in the upstream catchment and 300–850 mm in the downstream catchment (Hulsman et al. 2018). In the wet season in April, the monthly precipitation in the downstream catchment can be over 180 mm; while in the driest season in July, the minimum precipitation is less than 20 mm (World Weather & Climate Information 2022).

The socio-economic of the municipalities along the MRB is strongly dependent on the Mara River and its tributaries. The semi-intensive agricultural farming and animal husbandry are the main socio-economic activities (Roy et al. 2018; Das et al. 2022a). Wildlife tourism around the national forest park is the major economic industry pillar, accounting for a significant proportion of GDP and foreign exchange earnings. The tourist income improves the living conditions of residents and supports wildlife conservation in the MRB (WREM International Inc. 2008).

The rainfall pattern of MRB presents a bimodal regime and is considered to be the most complex in Africa (McClain et al. 2014). Associated with annual oscillations of the Intertropical Convergence Zone (ITCZ), the rainfall in MRB is controlled by the southward or northward migration of the ITCZ (Hulsman et al. 2018). The wet seasons are led on by ITCZ, which also causes short- and long-duration rainfall (Dessu and Melesse 2012; Das et al. 2022b). The seasonal variation is reflected by scarce rainfall in January–February (short-dry season), increased rainfall in March–May (long-wet season), decreased rainfall in June–September (long-dry season), and increased rainfall in October–December (short-wet season). The midstream of MRB is an important part of the Masai-Mara and Serengeti ecosystems and is the route of East African animal migration during the dry season.

Data

Based on the Moderate Resolution Imaging Spectroradiometer (MODIS) of the environmental remote sensing satellite Terra, the 16-day synthesized Level-3 MOD13Q1 product (Didan 2021a) and monthly MOD13A3 product (Didan 2021b) were used to obtain NDVI data. MOD13Q1 has the highest temporal resolution during the products of MODIS NDVI, which is a benefit to calculating time lags. The regions with cloud coverage were replaced by the climate records of the previous time series to achieve global cloud coverage. 23 images with spatial resolutions of 250 m were acquired each year (except 21 images in 2000) for process and analysis. MOD13A3 product was used to match the temporal resolution of precipitation data with a spatial resolution of 1000 m and was created by a time-weighted average of the 16-day 1-km products (Huete et al. 1999).

Monthly precipitation products of CHIRPS (Climate Hazards Group Infrared Precipitation with Stations) with a resolution of 0.05° (Funk et al. 2015) were selected to analyze the time lag of NDVI to seasonal precipitation. CHIRPS combines multi-data sources, taking advantage of in situ rain gauge measurements and long-term average satellite rainfall fields to derive climatological surfaces (Dinku et al. 2018). The original merging of station data was conducted at the pentad time scale, in which pentads were rescaled to generate other temporal resolution products. Its application has been confirmed and evaluated after being proposed (Chen et al. 2022; Duan et al. 2016; Zhong et al. 2019), as well as in East Africa (Dinku et al. 2018; Ayugi et al. 2021). To ensure the integrity of data, MOD13A3 and CHIRPS were selected from 2003 to 2022 since little data on MOD13A3 were missing before 2002.

Methods

Spatial and temporal trend analysis of NDVI

MOD13Q1 product was used to analyze the spatial and temporal variation in the MRB and obtain spatial variation at high resolution. The average value of NDVI was synthesized from 23 images each year, and the Anomaly Vegetation Index (AVI) was calculated to analyze the temporal variation (Chen et al. 1994). The anomalous value of NDVI reflects the inter-annual change of vegetation and indicates a bidirectional relationship with short-term climate characteristics. AVI can intuitively carry on the preliminary judgment of drought, which is reliable in areas that are highly dependent on precipitation, like MRB. The AVI could be expressed as (Yang et al. 2010):

$$AVI = NDVI_i - \frac{1}{n}\sum_{i=1}^{n} NDVI_i, \tag{1}$$

where $NDVI_i$ is the NDVI of each year, and n is the number of years. Similar to Eq. (1), the Anomaly Precipitation Index (API) was calculated at an annual scale to verify the vegetation's bidirectional indication of short-term climate characteristics. API could reflect the anomaly of precipitation and recognize its features:

$$API = Precipitation_i - \frac{1}{n}\sum_{i=1}^{n} Precipitation_i, \tag{2}$$

where $Precipitation_i$ is the precipitation of each year, and n is the number of years. Through unary linear regression analysis (Niu and Ni 2003; Liu et al. 2016), the spatial variation trend of NDVI of each year from 2001 to 2020 was calculated pixel by pixel. This method could be used to analyze the major trend of NDVI in the MRB and reduce the impact of extreme years. The calculation formula could be expressed as follows:

$$\theta = \frac{nV_i\sum_{i=1}^{n} i - \sum_{i=1}^{n} i\sum_{i=1}^{n} V_i}{n\sum_{i=1}^{n} i^2 - \left(\sum_{i=1}^{n} i\right)^2}, \tag{3}$$

where θ is the slope of trend change, n is the number of years, and V_i is the vegetation index of each year. The significance of the change in 20 years can be judged by the correlation degree between the year and the vegetation index.

Classification of spatial variation trends of NDVI

To directly reflect the difference in trends and calculate the area proportion, the trend results were reclassified into six categories according to the trend value and *P*-value (Table 1). The changes in NDVI around the basin could be compared, and spatial variation could be connected to the land cover types. Here, the *P*-value was used to judge the significance of the trend variation.

Table 1 The classification of spatial variation trend according to the trend value and *P*-value of NDVI based on unary linear regression analysis

Trend	Trend value	*P*-value
Decreased significantly	< 0	< 0.01
Decreased significantly	< 0	0.01–0.05
Decreased not significantly	< 0	> 0.05
Increased not significantly	> 0	> 0.05
Increased significantly	> 0	0.01–0.05
Increased significantly	> 0	< 0.01

Lag responses of NDVI response to seasonal precipitation by correlation analysis

Vegetation responds and adapts to seasonal changes under various climatic conditions. In the MRB, vegetation is more hydrologically resilient and sensitive to the water balance during dry seasons (Gan et al. 2021). In this study, two common methods were applied to calculate the lag time of NDVI response to seasonal precipitation. The first method was based on the correlation, while the second method was based on the mechanism of a seasonal alternation.

Generally, correlation analysis is the most common method to explore the relationship between variables. High correlation tends to be related to a strong association. The time lag of NDVI response to seasonal precipitation can be quantified by correlation analysis. The hysteretic relationship could be expressed as:

$$NDVI_{m+i} = k_i * Precipitation_m + b, \tag{4}$$

where $NDVI_{m+i}$ is the time series data of MOD13A3 from 2003 to 2022 for the same month expressed as m, i represents the lag month ranges from 0 to 3. $Precipitation_m$ is the corresponding time series data of the CHIRPS. For instance, when m represents January and considering 1-month lag ($i=1$), NDVI is the time series of February and precipitation is the time series of January; the time ranges of precipitation were set according to NDVI and the lag months. Here, k_i represents the linear regression coefficient, and b represents the constant term. We only consider a 3-month lag at most, 0-month represents no time lag. Since the time lag existed for the whole year, the analysis was conducted at a monthly scale in order to compare the seasonal differences.

Lag responses of NDVI to seasonal precipitation by seasonal alternations

Considering the seasonal variation of NDVI in the MRB, another method was applied to calculate the time lag and analyze the features of seasonal alternation. The average value of NDVI was calculated during each season based on the assumed lag time. The lag time can be inferred according to the changes in average values during 2001–2022. This method was based on seasonal alternation, which could provide a more accurate time lag. Here, a 16-day MOD13Q1 product was applied for the assumption. The lag time range was set from 0 to 60 days (the shortest season lasts 60 days), and the interval of lag time was set as 10 days. The average NDVI values were calculated within the corresponding season range, which could be expressed as:

$$f(t_1, t_2, t) = \overline{\sum_{i=t_1+t}^{t_2+t} NDVI_i}, \tag{5}$$

where t_1 is the start time of wet and dry seasons, t_2 is the end time of wet and dry seasons; t is the lag time; $NDVI_i$ is the average value of NDVI within the time range of $(t_1 + t, t_2 + t)$ of each year; $f(t_1, t_2, t)$ is the average value of NDVI within the corresponding wet and dry seasons under the lag time. The corresponding dates of t_1 and t_2 are shown in Table 2.

Lag responses of NDVI characteristic peaks to seasonal changes

In this section, we proposed characteristic peaks of NDVI and thus analyzed the time lag. In order to obtain NDVI changes of long time series, the average NDVI of each image was calculated. The spatiotemporal characteristics of peaks were discussed from the time range of seasonal changes. From the start of each wet/dry season to the end of the next dry/wet season (the range considering time lag), the extreme points of the corresponding seasons were marked as the characteristic peaks. They could be expressed as the maximum value points in the wet season and the minimum value points in the dry season. Each peak was named according to its season as follows: short-dry peak, long-wet peak, long-dry peak, and short-wet peak.

However, due to the response of NDVI to precipitation varied in seasons and reflected in the time lag of vegetation to reach the best or worst growth, the occurrence date of characteristic peaks might not be in the corresponding seasons.

Four characteristic peaks existed each year, and their variation characteristics were discussed. The time interval was calculated to characterize lag time according to the time range of characteristic peaks and the range of wet and dry seasons. The interval between the start and end of the time range could be expressed as $X_1 = t_{begin} - s_{begin}$ and $X_2 = t_{end} - s_{end}$, thus calculating the time lag:

$$peak_{timelag} = \frac{t_{end} + t_{begin}}{2} - \frac{s_{end} + s_{begin}}{2} = \frac{X_1 + X_2}{2}, \tag{6}$$

where X represents the time interval between the earliest/latest time and the start/end time of seasonal variation for four characteristic peaks, respectively; t_{begin} and

Table 2 Corresponding dates (month/day) of the start time (t_1) and end time (t_2) of four wet and dry seasons in the MRB

Season	Short-dry season	Long-wet season	Long-dry season	Short-wet season
t_1	1/1	3/1	6/1	10/1
t_2	2/29	5/31	9/30	12/31

t_{end} represent the earliest and latest time of characteristic peaks; s_{begin} and s_{end} represent the start and end times of the wet and dry seasons. The $peak_{timelag}$ reflects the lag time of NDVI characteristic peaks to the beginning of seasonal changes; it is an average interval between two ranges: the range of characteristic peaks and the range of the wet and dry seasons.

Results

Spatial and temporal variation of NDVI

The relatively dry or wet conditions from 2001 to 2020 were obtained by calculating the AVI and API. Results showed that the difference in annual NDVI was not obvious in most years. The short-term climate characteristics indicated by the anomaly values were reflected in the precipitation changes in the MRB. Negative anomaly values were significantly associated with insufficient precipitation. In Fig. 2, it was found that vegetation grew well during 2001, 2007, and 2020 while presenting a reversed trend during 2006, 2009, and 2017. The low AVI was mainly related to the precipitation in adjacent years. According to the API, rainfall in 2005 was extremely insufficient, while in 2006 was higher than average. This phenomenon resulted in a low NDVI in 2006 and a high NDVI in 2007, indicating that vegetation responded hysterically to precipitation. In 2009 and 2017, the lower API was consistent with lower AVI. The highest precipitation in 2020 coincided with the highest AVI from 2001 to 2020.

In order to analyze the spatial variation features of NDVI, the variation trend in the whole basin was obtained based on unary linear regression analysis. Areas that showed significant variation coincided with the land cover changes since a consistent trend from forest to cropland had been reported in the past years. The spatial variation trend of NDVI is shown in Fig. 3.

The trends showed that NDVI changed not significantly over 80% of areas, whereas the increase has not significantly occupied 60% of areas in the MRB. Almost 75% of areas presented an increased trend, and the areas increased significantly in several sub-basins. The land cover types were combined to illustrate the features of spatial trends. In the upstream, the increased trend areas were covered by savannas and cropland/natural vegetation mosaics of sub-basins 1 and 2. The increased trend areas were covered by grasslands of sub-basin 7 in the midstream and sub-basins 10, 11, and 12 in the

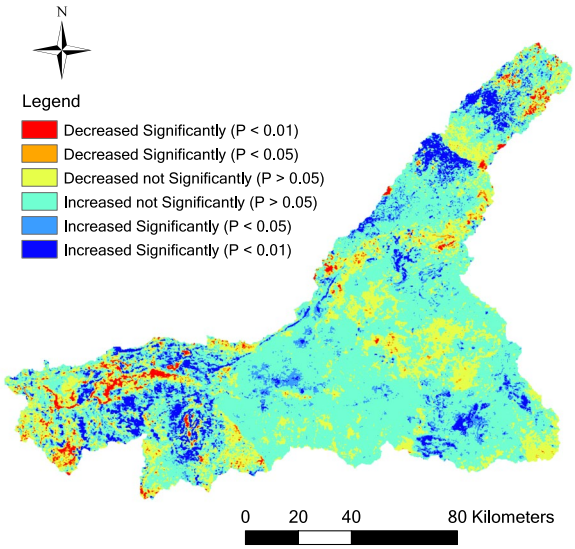

Fig. 3 Spatial variation trends of NDVI from 2001 to 2020 in the MRB

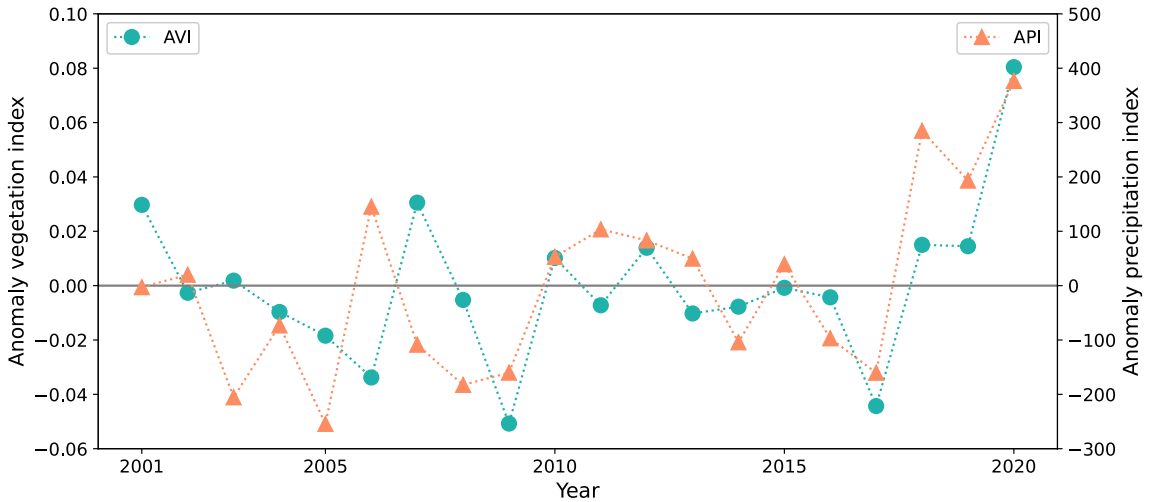

Fig. 2 Temporal variation of AVI and API from 2001 to 2020 in the MRB

downstream. Besides, the increased trend of NDVI near the northwest boundary of Masai-Mara National Reserve presented a distribution along the boundary.

Moreover, the areas that decreased significantly showed specific characteristics and occupied nearly 3.5% of the areas in the MRB. In the upstream, the decreased trend areas were covered by savannas, although they occupied only a few regions compared to the increased trend areas. In the downstream, part of the areas covered by grasslands and cropland presented a decreased trend in sub-basins 11 and 12, especially areas around the wetland. The analysis was carried out on the pixel level, and the pixel number and proportion of different trends is shown in Table 3.

Table 3 NDVI change trend and pixel proportion from 2001 to 2020 in the MRB

Change trend	Proportion (%)
Decreased significantly ($P<0.01$)	1.89
Decreased significantly ($P<0.05$)	1.73
Decreased not significantly ($P>0.05$)	21.53
Increased not significantly ($P>0.05$)	60.08
Increased significantly ($P<0.05$)	7.86
Increased significantly ($P<0.01$)	6.91

Time lag of NDVI response to seasonal precipitation

Time lag of NDVI response to seasonal precipitation based on correlation analysis

Regression analysis showed that the maximum correlation of time lag between NDVI and precipitation was considered the most reliable. The corresponding lag month was regarded as the lag time. The time lag of NDVI response to precipitation in the MRB during each month is shown in Fig. 4. Considering the significance of the correlation coefficient, grids whose *P*-value were greater than 0.05 were depicted in grey in Fig. 4, yellow in Fig. 5, and not included in the analysis.

From the perspective of time lag effects, the lag month presented spatiotemporal heterogeneity in the MRB. One-month lag effect dominated in January, May, and November; the 2-month lag effect dominated in February and March. Due to the lack of valid values, features of some months could not be detected especially in the

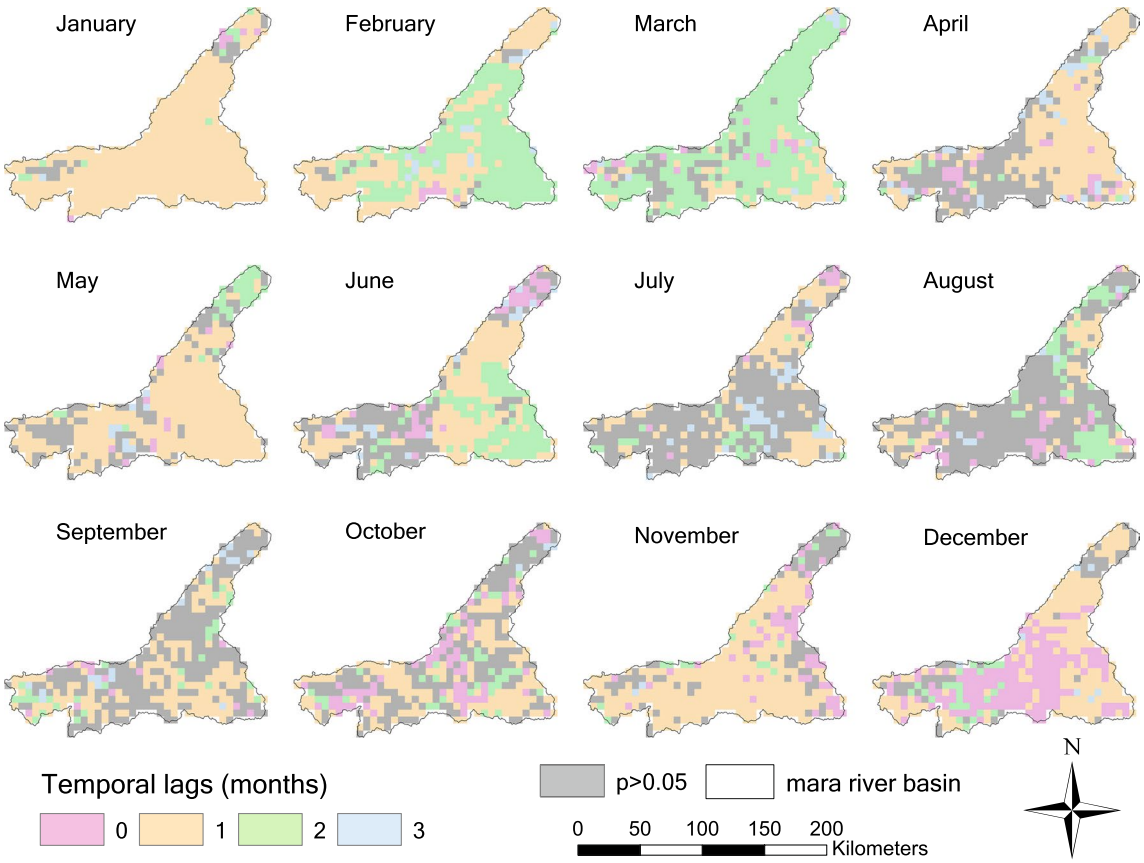

Fig. 4 Lag time (0–3 months) of NDVI response to precipitation and spatial variation over months on the pixel scale in the MRB

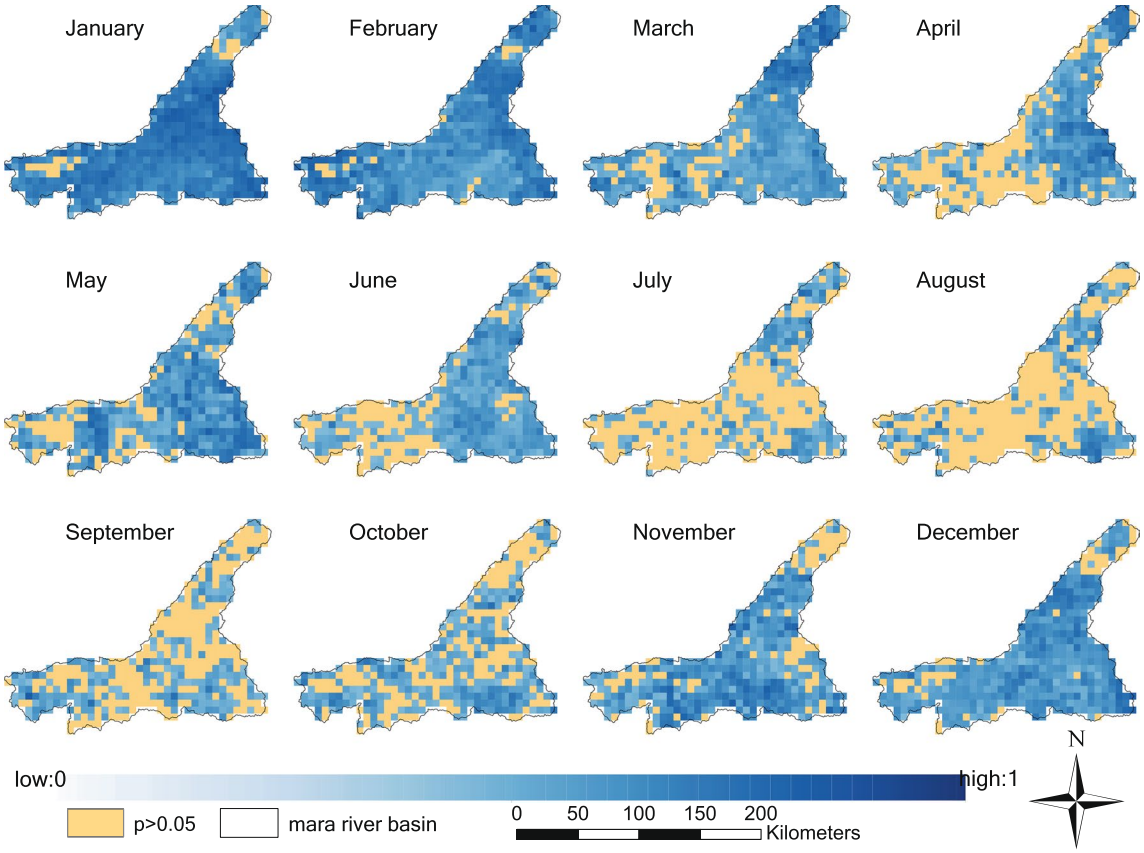

Fig. 5 Maximum correlation corresponded to the time lag of NDVI response to precipitation and spatial variation over months on the pixel scale in the MRB

dry seasons from June to September. In addition, the 1-month lag effect was obvious in April, July, September, and October. In June, the 1-month lag effect took effect mainly located upstream near Mau forest, while the 2-month lag effect appeared in the east of midstream. Most pixels were not available in August. No lag effect took up almost half areas in December mainly in the middle of MRB, while the 1-month effect took up in the east. December was the rare month when no lag effect took effect, as well as when the spatial variation of time lag was the most salient. The time lag statistics of valid pixels are shown in Table 4. Almost all months presented a 1-month lag effect, except February and March which presented closer to the 2-month lag effect. Mean and median months of time lag showed similar features.

The longer time lag in February and March might be related to the short-dry season. To meet the ecological water demand of the vegetation, the vegetation would be affected by longer periods of insufficient precipitation in the dry season. In general, the time lags of dry seasons were longer, especially in long-dry season when lacking

Table 4 The statistical values of the lag response of NDVI to precipitation over months in the MRB, including the lag time, correlation, and number of valid pixels that pass the significance test

Month	Number of valid pixels (*P*-value ≤ 0.05)	Average month	Median month	Average correlation
January	412	1.01	1	0.70
February	418	1.58	2	0.65
March	381	1.76	2	0.60
April	286	1.14	1	0.58
May	343	1.11	1	0.61
June	321	1.30	1	0.55
July	181	1.42	1	0.54
August	168	1.26	1	0.55
September	208	1.24	1	0.53
October	264	0.90	1	0.55
November	353	0.91	1	0.60
December	387	0.67	1	0.61

precipitation from July to September. However, time lags were not as long as that of February to March, still longer than the wet seasons. This phenomenon was related to the number of valid pixels. During the long-dry seasons, vegetation responded physiologically to a continuous lack of precipitation. This caused the test results to be insufficient to support the correlation analysis between NDVI and precipitation, resulting in less than half of the pixels being available in this season. Seasonal variation also affected the time lag of vegetation through varied precipitation.

The maximum correlation corresponding to the lag month is shown in Fig. 5. Generally, the correlation was higher than 0.44, and the maximum surpassed 0.85. A good correlation demonstrated the effectiveness of time lag, especially in January. Average correlations in the wet seasons were higher than those in the dry seasons since the long-dry season showed a lower correlation compared with other months. The results of the average correlation of each month are shown in Table 4.

Time lag of NDVI response to seasonal precipitation based on the mechanism of seasonal alternation

Rainfall lasted a long time in the MRB during the long-wet season and improved vegetation growth conditions with sufficient precipitation. The precipitation was seriously insufficient in the long-dry season, and vegetation was in a state of water shortage. Precipitation in the short-wet season was no more sufficient than long-wet season, and vegetation experienced a gradual recovery from the long-dry season with slightly worse growth. NDVI in the short-wet season was lower than that of the long-wet season but higher than that of the short-dry season. During the short-dry season, the precipitation was reduced. The vegetation showed slightly arid but could still maintain greenness for a period due to the influence of the last wet season and the growth mechanism of vegetation. Vegetation grew better in the wet seasons than that of the dry seasons. According to different time lags, the average values of NDVI divided into wet and dry seasons were plotted.

Figure 6 illustrates the highest NDVI in the long-wet season and the lowest NDVI in the long-dry season. However, the NDVI of the short-wet and short-dry seasons were not that far apart when time lag was considered. In the alternation of seasonal changes, the complete effect of rainfall on vegetation was reflected. The NDVI of the wet season was higher than that of the dry season. The time required for this process was the lag time, which could be thought of as when the NDVI of the short-wet season was close to that of the short-dry season. Results showed that the requirement was satisfied when the lag time was 20–40 days, and 30 days was almost the dividing line and thus was considered to be the suitable lag time in the MRB. The conclusion was consistent with the previous one in "Time lag of NDVI response to seasonal precipitation based on correlation analysis" section.

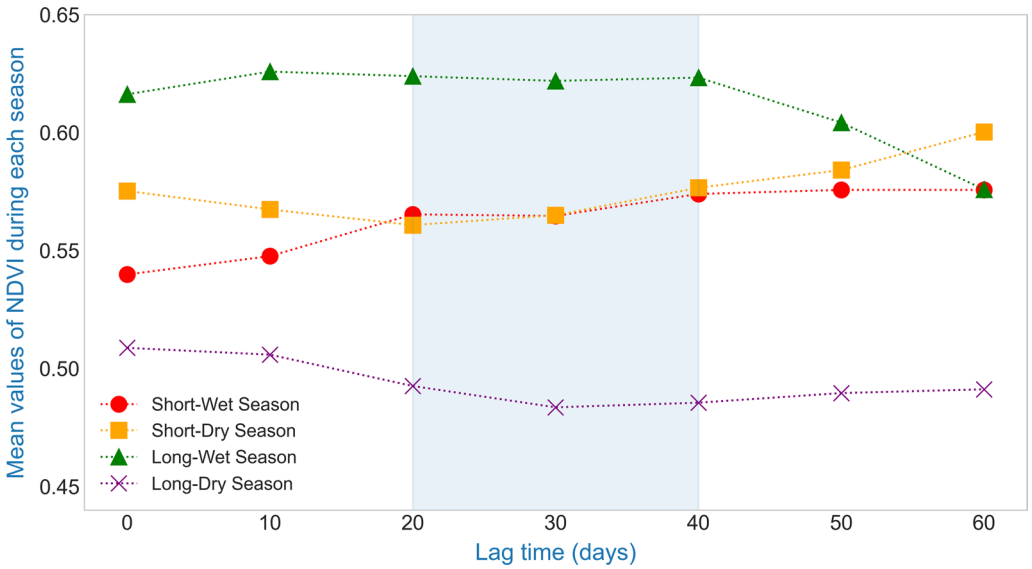

Fig. 6 Variation of mean NDVI of wet and dry seasons at 10-day intervals within the assumed lag time range from 0 to 60 days. The blue shadows indicate situations where the mean NDVI in the short-wet season was close to that of the short-dry season

Time lag of NDVI characteristic peaks response to seasonal variation

The features of wet and dry seasons lead to four characteristic peaks of NDVI, and the four peaks reflected the response of NDVI to seasonal variation. By calculating the mean value of each image, the long-time series of NDVI is plotted and shown in Fig. 7. The first day of each year (in 2000 was the date of the first available data) was marked on the horizontal axis.

The long-time series diagram showed that each year was accompanied by a sharp change in the mean value of NDVI, which formed an upward short-wet peak, followed by a downward short-dry peak, and then formed an upward long-wet peak again. After experiencing a shock in the middle of the year, it formed a downward long-dry peak. The four upward or downward peaks had the characteristics of a single peak or two similar double peaks, only to be recognized as the first one.

Generally, four peaks had annual characteristics and appeared alternately. Figure 7 shows the positions of four characteristic peaks in the past 20 years. The occurrence times of the short-wet peak, short-dry peak, and long-wet peak were concentrated on 12/2–1/17, 1/17–4/7, and 4/7–6/26. Long-dry peak appeared over a longer time horizon, and the occurrence time was 7/27–11/1. Long-dry peak fluctuated greatly from the end of July to the beginning of January of the next year from 2001 to 2009, which was related to the longest dry season. After 2010, the long-dry peak was relatively stable from the end of July to the end of September, only delayed in 2015, which may be related to the severe drought at the end of 2016.

In Fig. 8, the gray lines represent the time range of wet and dry seasons, and the red dashed lines represent the time range of the characteristic peaks. For visual display in the mapping, the following parameters corresponded to the X_1 and X_2: a_1, b_1, c_1, and d_1 represented the intervals from the start time of seasons to the earliest time range of four peaks; a_2, b_2, c_2, and d_2 represented the intervals from the end time of seasons to the latest time range of four peaks. Due to the severe drought, there was a systematic deviation in 2006, so the NDVI characteristic peaks of 2006 were not considered when calculating the time range.

The results from Table 5 showed that the longer the duration of seasons, the greater the difference between the time range of peaks and the values of seasonal peak_timelag. The time lag of the four peaks varied slightly, and the average lag time from the start of the seasons to the appearance of the characteristic peaks was 35.5 days.

The values of four characteristic peaks varied greatly with time (Fig. 9), as well as a sensitive indicator for drought. According to AVI, insufficient precipitation was captured by the long-wet peak in 2006, the long-dry peak in 2009, and peaks short-wet peak, short-dry peak, and long-wet peak in 2017. Short-wet and short-dry peaks showed high values during 2001, 2007, and 2020, consistent with AVI.

Discussion

Temporal and spatial variation of NDVI characteristics

The AVI outliers could be used to deduce obvious wetness or drought at the annual scale. The negative values in 2006, 2009, and 2017 indicated the severe drought that might be caused by insufficient precipitation, corresponding to the low levels of rivers (Dybas 2011). Since vegetation lags behind seasonal precipitation, the precipitation from the preceding year could have an impact. The average monthly precipitation for the short-wet season

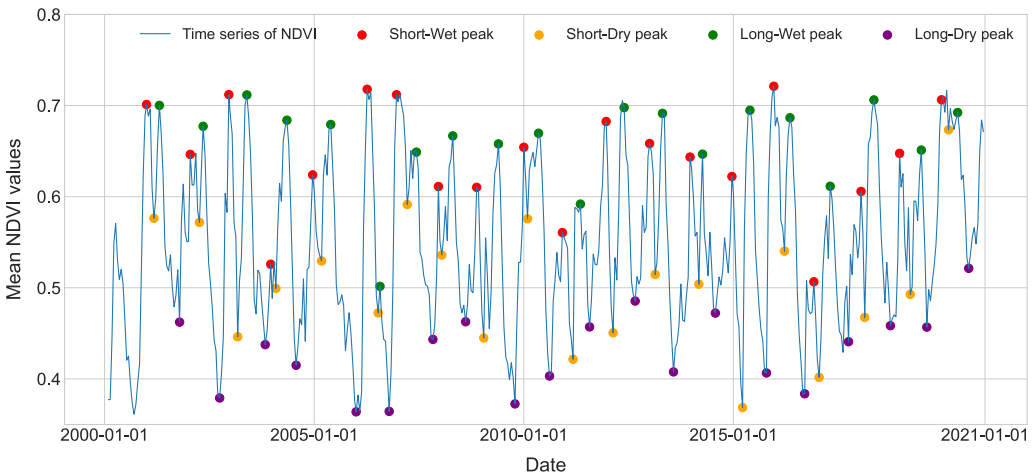

Fig. 7 Four NDVI characteristic peaks and their time distributions during the long time series of NDVI from 2000 to 2020 in the MRB. Peaks in 2000 were not plotted due to missing data for January

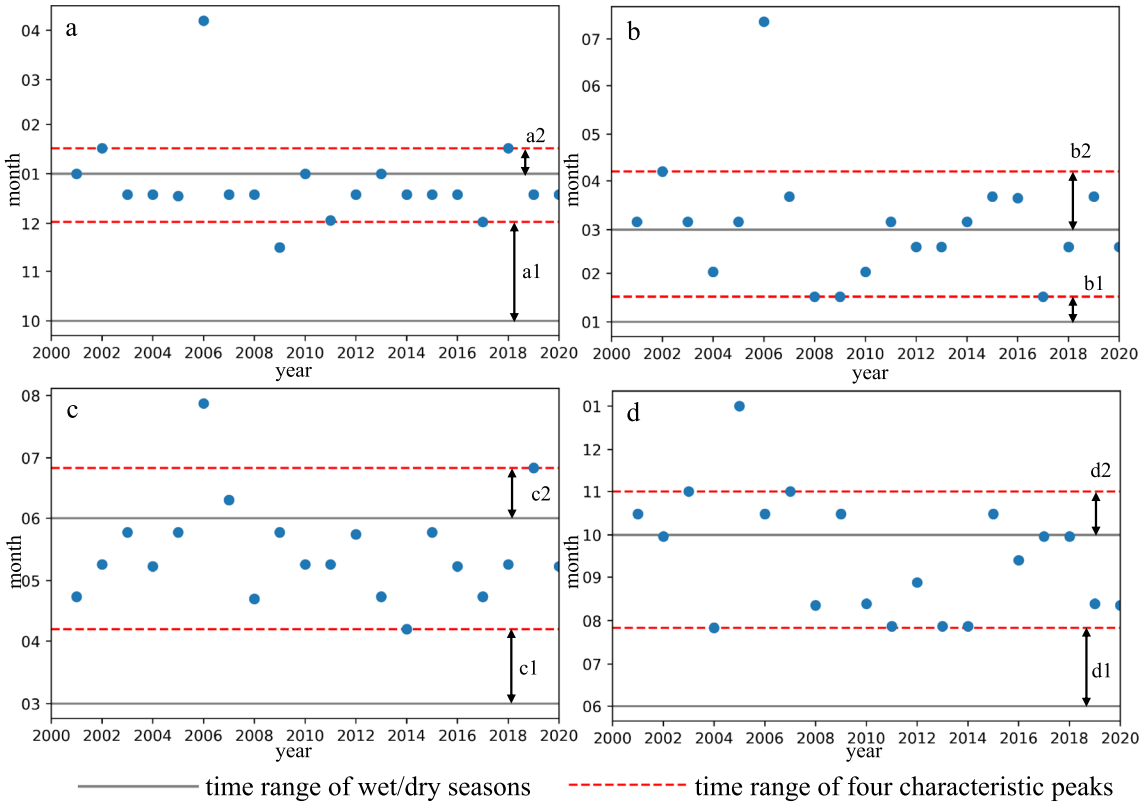

Fig. 8 Time distributions of four NDVI characteristic peaks from 2001 to 2020, and intervals between the start/end of four seasons and corresponding NDVI characteristic peaks: **a** short-wet peak, **b** short-dry peak, **c** long-wet peak, and **d** long-dry peak

Table 5 The statistical values of time lag of NDVI characteristic peaks to seasonal variation, including duration of each season, intervals between the start/end of the season and NDVI characteristic peaks, and the peak_timelag (unit: days)

Peak	Season duration	$X_i(i=1,2)$	Value	pea{k}_{timelag}	Total average
Short-wet peak	90	a_1	62	39	35.5
		a_2	16		
Short-dry peak	60	b_1	16	27	
		b_2	38		
Long-wet peak	90	c_1	37	32	
		c_2	27		
Long-dry peak	120	d_1	56	44	
		d_2	32		

was just 49.78 mm at the end of 2005, but it increased to 160.57 mm by the end of 2006. That made it clear how the previous year's precipitation affected the NDVI of the following year and showed how the two factors interacted. In 2009 and 2017, the precipitation was less than the average from January to May, related to the low NDVI. The shortage of precipitation in 2017 influenced NDVI in 2018, even if precipitation was sufficient from 2018 to 2020. The vegetation's lag response to precipitation was a representation of the intricate process within the ecosystem, and this sustained impact necessitated quantifying the lag impact. The precipitation in 2018 was concentrated in the long-wet season, while the short-wet season at the end of 2019 saw the most precipitation. Due to the occurrence time of seasonal precipitation, the lag response led to extraordinarily high values of AVI and NDVI in 2020 but not in 2019. In 2020, precipitation was consistently greater than the average, especially during

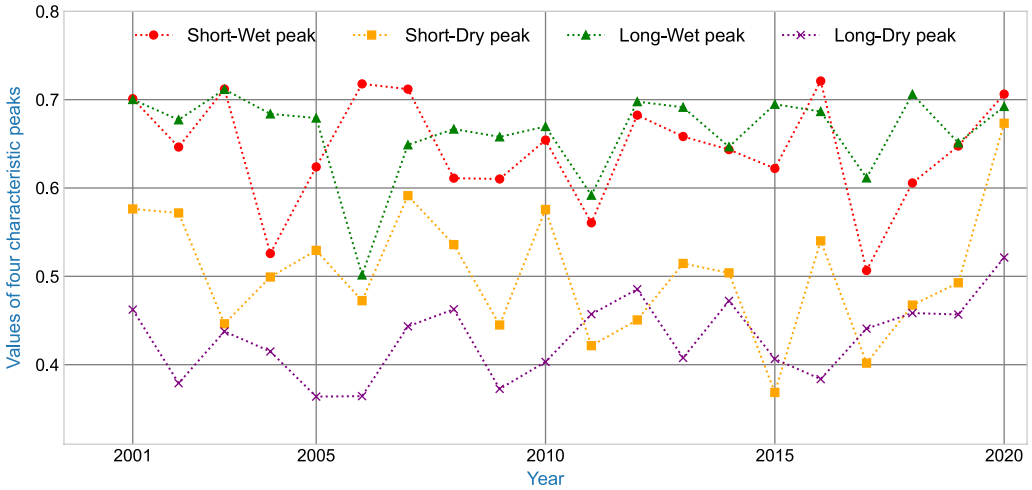

Fig. 9 The values of four NDVI characteristic peaks from 2001 to 2020: **a** short-wet peak, **b** short-dry peak, **c** long-wet peak, and **d** long-dry peak

the wet seasons, which provided favorable conditions for the growth of plants. These events demonstrated the efficiency of time lag by illustrating the dynamic effects of time distribution of seasonal precipitation on the vegetation growth process.

In most regions, the NDVI did not change significantly from a spatial perspective, and the major feature was the increased trend. In the upstream, areas surrounding the Mau Forest were favorable for agriculture. The decreased trend was related to the expansion of small-scale agriculture, which was the main type. The situation was similar downstream, where there was a concentration of wetlands and grasslands. Land use in the MRB has significantly changed (Mwangi et al. 2017) since the end of the last century, which negatively impacts vegetation from the performance of extremely dry or wet years.

Although there were frequent droughts in the MRB, precipitation had not drastically decreased in recent years. Gradient precipitation existed in different sub-basins, and the difference between wet seasons and dry seasons might be larger. According to models and predictions of water resource supply coupled with climate change (Kumar et al. 2014), water availability in the MRB will continue to rise during the wet seasons and fall during the dry ones in the coming decades. The seasonal fluctuations in vegetation that interact with human activities would be more impacted by this tendency. Population migration to catchments in search of water resources was connected with an increase in human demand for food and water resources (Mati et al. 2008), as well as the change in NDVI features near the wetland. Deforestation, animal husbandry, and agricultural land expansion were on the rise for subsistence purposes, which had negative impacts that were reflected in the spatiotemporal characteristics of NDVI trends.

Lag responses of NDVI to seasonal changes

The lag effect of NDVI to seasonal precipitation was analyzed from a statistical perspective. The results considered the time lag at a monthly scale and revealed that there were geographical and temporal variations in the lag response of NDVI to precipitation. The seasonal characteristics of precipitation were affected by climatic conditions in various regions and were significantly related to the variation of the lag effect. In addition, the time lag was analyzed from the perspective of seasonal changes and was consistent with the average time lag obtained by statistics. The statistical method was limited by the temporal resolution of data, while the time lag obtained from the seasonal changes could be more flexible.

According to the alternation of seasons, the fact that NDVI of wet seasons was stably higher than that of dry seasons was utilized to obtain lag time. Deviation existed in the 10-day interval since the calculation was based on 16-day NDVI, but the results were still very convincing. Shorter interval and high-resolution NDVI data will be used to calculate the time lag, which is more precise. However, the lag time varies greatly from year to year, and an average time that can fully reflect the lag is more valuable. According to the results, the time lag of NDVI to seasonal precipitation was about 30 days in the MRB which was consistent with the existing study (Wu et al. 2015). The variation at the monthly scale was still outstanding and worth further study since complex precipitation behaviors on terrestrial vegetation had been found (Wen et al. 2019).

In this study, the accurate lag time still existed deviations at a monthly scale, and higher temporal resolution data shall solve this problem. The geographic difference has not been explained. For example, no lag effect showed in the middle basin in December, while there was a 1-month lag in the upper areas. The primary factor and the mechanism that resulted in the situation would be detected from the perspective of rainfall patterns and soil's physical and chemical properties. Besides, the accumulative effect of precipitation on NDVI (Jiang et al. 2022) was not considered. The land cover related to vegetation might have changed due to human activities, which will influence the time lag of NDVI (Kong et al. 2020). Detailed influence of accumulative effect and land cover types could be compared with a time lag in the future.

Lag responses of NDVI characteristic peaks to seasonal changes

This study proposed four NDVI characteristic peaks and examined their values and occurrence time in the MRB. The MRB presented a bimodal rainfall pattern, reflecting the alternation of seasons. Four typical peaks were deemed appropriate to depict the seasonal variation of the wet and dry seasons in light of the aspects of seasonal changes. The short-wet peak appeared at the end of each year, and its value fluctuated greatly under the influence of the long-dry season. The short-dry peak reflected a transition from the short-wet season to the long-wet season, with a slight decrease in NDVI. Long-wet peak symbolized the most abundant rainfall for vegetation growth, which was usually reflected in the annual maximum NDVI. Long-dry peak represented the driest time and the longest season of each year.

The time lag based on the difference between NDVI characteristic peaks and the time range of seasonal variation represents the stabilization effect of the wet and dry seasons on vegetation growth. The lag time of wet seasons represents the accumulation of rainfall that makes vegetation grow best, while that of dry seasons is when continuous drought makes vegetation grow worst. The average value of NDVI in the MRB varied from 0.4 to 0.7 over time. When a persistent drought appeared, the position of four NDVI characteristic peaks would decrease significantly. The general status of drought features, vegetation growth, and animal movement in the MRB could be thoroughly studied. The vegetation recovery after drought could also be assessed according to the periods and values of four peaks.

Four peak_timelags were special because they represented the lag effect of wet or dry seasons. Time lag took effect differently during each season, and the lag time could vary more than 10 days. But the duration of different seasons could vary by up to 2 months. So the average time lag of 35.5 days aimed to show the general time lag and the difference in each season still existed.

Since the characteristic peaks represent the maximum or minimum values of NDVI in the corresponding seasons, the time lag varies in different seasons. In general, the longer the season range, the longer the time lag. The mean time lag was slightly more than one month, consistent with the results of statistical and seasonal mechanisms. The values of NDVI characteristic peaks also captured the drought and wetness represented by AVI, but the exact relationship between the four peaks and the AVI needed to be further studied. The growth of vegetation indicated by NDVI characteristic peaks may also be affected by other natural or human factors, which should be considered in the future.

Conclusions

AVI and unary linear regression analysis were used to investigate the temporal and spatial variation characteristics of NDVI in the MRB. AVI showed trends for drought conditions in 2006, 2009, and 2017 and for wet conditions in 2001, 2007, and 2020. The API demonstrated plants' lag response and proved AVI's accuracy in detecting wetness and drought. From 2001 to 2020, NDVI presented an increasing trend in most regions, although almost 60% of areas of MRB increased not significantly. In the downstream of the MRB, the change trends were most obvious compared with other areas, reflecting the influence of human activities. The decreased trend areas were mainly covered by savannas close to the human-inhabited area.

Two methods were applied to explore the time lag of NDVI to seasonal precipitation. Correlation analysis showed that the 1-month lag effect dominated in most months, with February and March showing more of a 2-month lag effect. The seasonal variation and the time lag led to different spatial patterns among months. The lag time of NDVI to the changes between wet and dry seasons was examined and was considered to be 30 days.

Four NDVI characteristic peaks were found to be an efficient way to describe the seasonal characteristics of average NDVI. After examining the timing of the characteristic peaks and the various seasons, the findings revealed an average time lag of 35.5 days between each seasonal change to the characteristic peak. The rationality and meaning of NDVI characteristic peaks were clear, which could better capture seasonal variation.

It is challenging to enable the monitoring of short time intervals, long time ranges, and broad areas due to the absence of infrastructure construction in the MRB. The vegetation in the basin is extremely sensitive to variations in the wet and dry seasons, and water resources are

in short supply. Water resources need to be managed rationally according to lag response for the utilization of water resources by human activities, which should be in harmony with the development of the ecological environment. The meaningful exploration provides a new perspective to study the variation characteristics of wet and dry seasons in the basin.

Abbreviations

AVI	Anomalous Vegetation Index
API	Anomaly Precipitation Index
ITCZ	Intertropical Convergence Zone
MRB	Mara River Basin
MODIS	Moderate Resolution Imaging Spectroradiometer
NDVI	Normalized Difference Vegetation Index
CHIRPS	Climate Hazards Group Infrared Precipitation with Stations

Acknowledgements
Not applicable.

Author contributions
ZZ and SF designed the study; SF and SZ collected the data; XG, PD, and WZ contributed to the data analysis and manuscript writing. All authors read and approved the final manuscript.

Funding
This work was supported by the National Key R&D Program of China [Grant Number 2018YFE0105900].

Availability of data and materials
The datasets analyzed during the current study are available in the CHIRPS repository, https://data.chc.ucsb.edu/products/CHIRPS-2.0/, and in the MODIS repository, https://search.earthdata.nasa.gov/search.

Declarations

Ethics approval and consent to participate
Not applicable.

Consent for publication
Not applicable.

Competing interests
The authors declare that they have no competing interests.

Received: 10 April 2023 Accepted: 27 September 2023
Published online: 04 October 2023

References

Ayugi B, Zhihong J, Zhu H et al (2021) Comparison of CMIP6 and CMIP5 models in simulating mean and extreme precipitation over East Africa. Int J Climatol 41:6474–6496. https://doi.org/10.1002/joc.7207

Birundu AM, Mutua BM (2017) Analyzing the Mara River Basin behaviour through rainfall-runoff modeling. Int J Geosci 8:1118–1132. https://doi.org/10.4236/ijg.2017.89064

Cao M, Woodward FI (1998) Dynamic responses of terrestrial ecosystem carbon cycling to global climate change. Nature 393:249–252. https://doi.org/10.1038/30460

Chamaille-Jammes S, Fritz H, Murindagomo F (2006) Spatial patterns of the NDVI–rainfall relationship at the seasonal and interannual time scales in an African savanna. Int J Remote Sens 27:5185–5200. https://doi.org/10.1080/01431160600702392

Chen W, Xiao Q, Sheng Y (1994) Application of anomalous vegetation index in monitoring extreme drought in 1992. Remote Sens Environ 2:106–112

Chen Z, Wang W, Fu J (2020) Vegetation response to precipitation anomalies under different climatic and biogeographical conditions in China. Sci Rep 10:830. https://doi.org/10.1038/s41598-020-57910-1

Chen S, Li Q, Zhong W et al (2022) Improved monitoring and assessment of meteorological drought based on multi-source fused precipitation data. Int J Env Res Pub Health 19:1542. https://doi.org/10.3390/ijerph19031542

Das P, Zhang Z, Ren H (2022a) Evaluating the accuracy of two satellite-based Quantitative Precipitation Estimation products and their application for meteorological drought monitoring over the Lake Victoria Basin, East Africa. Geo-Spat Info Sci 25:500–518. https://doi.org/10.1080/10095020.2022.2054731

Das P, Zhang Z, Ren H (2022b) Evaluation of four bias correction methods and random forest model for climate change projection in the Mara River Basin, East Africa. J Water Clim Change 13:1900–1919. https://doi.org/10.2166/wcc.2022.299

Dessu SB (2013) Water Demand and Allocation in the Mara River Basin, Kenya/Tanzania in the Face of Land Use Dynamics and Climate Variability. Doctor of Philosophy Geosciences, Florida International University

Dessu SB, Melesse AM (2012) Impact and uncertainties of climate change on the hydrology of the Mara River basin, Kenya/Tanzania. Hydrol Process 27:2973–2986. https://doi.org/10.1002/hyp.9434

Didan K (2021a) MODIS/Terra vegetation indices 16-Day L3 Global 250m SIN Grid V061, NASA EOSDIS land processes distributed active archive center. https://doi.org/10.5067/MODIS/MOD13Q1.061. Accessed 17 Sep 2023.

Didan K (2021b) MODIS/Terra vegetation indices monthly L3 Global 1km SIN Grid V061, NASA EOSDIS land processes distributed active archive center. https://doi.org/10.5067/MODIS/MOD13A3.061. Accessed 17 Sep 2023.

Dinku T, Funk C, Peterson P et al (2018) Validation of the CHIRPS satellite rainfall estimates over eastern Africa. Quart J Royal Meteoro Soc 144:292–312. https://doi.org/10.1002/qj.3244

Duan Z, Liu J, Tuo Y et al (2016) Evaluation of eight high spatial resolution gridded precipitation products in Adige Basin (Italy) at multiple temporal and spatial scales. Sci Total Environ 573:1536–1553. https://doi.org/10.1016/j.scitotenv.2016.08.213

Dybas CL (2011) Saving the Serengeti-Masai Mara. Bioscience 61:850–855. https://doi.org/10.1525/bio.2011.61.11.4

Funk C, Peterson P, Landsfeld M et al (2015) The climate hazards infrared precipitation with stations—a new environmental record for monitoring extremes. Sci Data 2:150066. https://doi.org/10.1038/sdata.2015.66

Gan G, Liu Y, Sun G (2021) Understanding interactions among climate, water, and vegetation with the Budyko framework. Earth Sci Rev 212:103451. https://doi.org/10.1016/j.earscirev.2020.103451

He Q (2019) Spatio-temporal variation of NDVI and its response to meteorological factors in pearl river delta based on MODIS data. Ecol Environ Sci 28:1722–2130

Huete A, Justice C, van Leeuwen W (1999) MODIS vegetation index (Mod 13) algorithm theoretical basis document, version 3

Hulsman P, Bogaard TA, Savenije HHG (2018) Rainfall-runoff modelling using river-stage time series in the absence of reliable discharge information: a case study in the semi-arid Mara River basin. Hydrol Earth Syst Sci 22:5081–5095. https://doi.org/10.5194/hess-22-5081-2018

Jaber SH, Al-Saadi LM, Al-Jiboori MH (2020) Spatial vegetation growth and its relation to seasonal temperature and precipitation in Baghdad. Int J Agric Stat Sci 16(1):2021–2026

Jeong S-J, Schimel D, Frankenberg C et al (2017) Application of satellite solar-induced chlorophyll fluorescence to understanding large-scale variations in vegetation phenology and function over northern high latitude forests. Remote Sens Environ 190:178–187. https://doi.org/10.1016/j.rse.2016.11.021

Jiang L, Jiapaer G, Bao A et al (2017) Vegetation dynamics and responses to climate change and human activities in Central Asia. Sci Total Environ 599–600:967–980. https://doi.org/10.1016/j.scitotenv.2017.05.012

Jiang W, Niu Z, Wang L et al (2022) Impacts of drought and climatic factors on vegetation dynamics in the Yellow River Basin and Yangtze River Basin, China. Remote Sens 14:930. https://doi.org/10.3390/rs14040930

Kong D, Miao C, Wu J et al (2020) Time lag of vegetation growth on the Loess Plateau in response to climate factors: Estimation, distribution, and

influence. Sci Total Environ 744:140726. https://doi.org/10.1016/j.scitotenv.2020.140726
Kraft B, Jung M, Körner M et al (2019) Identifying dynamic memory effects on vegetation state using recurrent neural networks. Front Big Data 2:31. https://doi.org/10.3389/fdata.2019.00031
Kumar S, Lawrence DM, Dirmeyer PA, Sheffield J (2014) Less reliable water availability in the 21st century climate projections. Earth's Future 2:152–160. https://doi.org/10.1002/2013EF000159
Liu Y, Li C, Liu Z, Deng X (2016) Spatial-temporal variation of vegetation cover in Xinjiang based on GIMMS-NDVI from 1982 to 2013. Acta Ecol Sin 36:6198–6208
Mati BM, Mutie S, Gadain H et al (2008) Impacts of land-use/cover changes on the hydrology of the transboundary Mara River, Kenya/Tanzania. Lakes Reservoirs 13:169–177. https://doi.org/10.1111/j.1440-1770.2008.00367.x
McClain ME, Subalusky AL, Anderson EP et al (2014) Comparing flow regime, channel hydraulics, and biological communities to infer flow–ecology relationships in the Mara River of Kenya and Tanzania. Hydrol Sci J 59:801–819. https://doi.org/10.1080/02626667.2013.853121
Mwangi H, Lariu P, Julich S et al (2017) Characterizing the intensity and dynamics of land-use change in the Mara River Basin, East Africa. Forests 9:8. https://doi.org/10.3390/f9010008
Niu Z, Ni S (2003) Remote sensing monitoring model of grassland vegetation biomass around Qinghai Lake. Acta Geogr Sin 58:695–702
Pang G, Wang X, Yang M (2017) Using the NDVI to identify variations in, and responses of, vegetation to climate change on the Tibetan Plateau from 1982 to 2012. Quatern Int 444:87–96. https://doi.org/10.1016/j.quaint.2016.08.038
Piao S, Fang J (2003) Seasonal differences in response of terrestrial vegetation to climate change in China from 1982 to 1999. Acta Geogr Sin 58:119–125
Roy T, Valdés JB, Lyon B et al (2018) Assessing hydrological impacts of short-term climate change in the Mara River basin of East Africa. J Hydrol 566:818–829. https://doi.org/10.1016/j.jhydrol.2018.08.051
Tang Z, Ma J, Peng H et al (2017) Spatiotemporal changes of vegetation and their responses to temperature and precipitation in upper Shiyang River Basin. Adv Space Res 60:969–979. https://doi.org/10.1016/j.asr.2017.05.033
Tucker CJ (1979) Red and photographic infrared linear combinations for monitoring vegetation. Remote Sens Environ 8:127–150. https://doi.org/10.1016/0034-4257(79)90013-0
Wen Y, Liu X, Xin Q et al (2019) Cumulative effects of climatic factors on terrestrial vegetation growth. J Geophys Res Biogeosci 124:789–806. https://doi.org/10.1029/2018JG004751
World Weather & Climate Information (2022) Climate in Musoma (Mara region), Tanzania
WREM International Inc. (2008) Mara River Basin Monograph, Mara River Basin transboundary integrated water resources management and development project, Final Technical Report. Atlanta
Wu D, Zhao X, Liang S et al (2015) Time-lag effects of global vegetation responses to climate change. Glob Change Biol 21:3520–3531. https://doi.org/10.1111/gcb.12945
Xu L, Myneni RB, Chapin FS III et al (2013) Temperature and vegetation seasonality diminishment over northern lands. Nat Clim Change 3:581–586. https://doi.org/10.1038/nclimate1836
Yang T, Gong H, Li X et al (2010) Research progress of soil moisture monitoring by remote sensing. Acta Ecol Sin 30:6264–6277
Zhang G, Zhang Y, Dong J, Xiao X (2013) Green-up dates in the Tibetan Plateau have continuously advanced from 1982 to 2011. Proc Natl Acad Sci USA 110:4309–4314. https://doi.org/10.1073/pnas.1210423110
Zhao W, Zhao X, Zhou T et al (2017) Climatic factors driving vegetation declines in the 2005 and 2010 Amazon droughts. PLoS ONE 12:e0175379. https://doi.org/10.1371/journal.pone.0175379
Zhong R, Chen X, Lai C et al (2019) Drought monitoring utility of satellite-based precipitation products across Mainland China. J Hydrol 568:343–359. https://doi.org/10.1016/j.jhydrol.2018.10.072
Zhu W, Zhang Z, Zhao S et al (2022) Vegetation greenness trend in dry seasons and its responses to temperature and precipitation in Mara River Basin, Africa. Int J Geo-Infor 11:426. https://doi.org/10.3390/ijgi11080426

Publisher's Note